Antibacterial activity of silver nanoparticles synthesized from *Persicaria odorata* (L.) sojak leaves extract

Cite as: AIP Conference Proceedings **2353**, 030022 (2021); https://doi.org/10.1063/5.0052607
Published Online: 25 May 2021

Faridah Aminullah, Nik Ahmad Nizam Nik Malek and Khairunadwa Jemon

Antibacterial Activity of Silver Nanoparticles Synthesized from *Persicaria odorata* (L.) Sojak Leaves Extract

Faridah Aminullah[1], Nik Ahmad Nizam Nik Malek[2], and Khairunadwa Jemon[1,a]

[1]*Department of Biosciences, Faculty of Sciences, Universiti Teknologi Malaysia, 81310 Skudai, Johor, Malaysia*
[2]*Centre for Sustainable Nanomaterials (CSNano), Ibnu Sina Institute for Scientific and Industrial Research (ISI-ISIR), Universiti Teknologi Malaysia, 81310 UTM, Johor, Malaysia*

[a]Corresponding author: khairun_nadwa@utm.my

Abstract. Recent findings suggested that plant-mediated synthesized silver nanoparticles exhibit significant antibacterial property, yet the exact mechanisms and toxicity remain unraveled. Hence, this present study aims to utilize the leaves extract from *Persicaria odorata* (L.) Sojak as the reducing agent for the fabrication of silver nanoparticles (PO-AgNPs) and to evaluate their antibacterial properties. The formation of PO-AgNPs was verified by ultraviolet-visible (UV-Vis) spectrophotometer which revealed an absorption peak at around 440 nm. Further characterization using Fourier transform infrared (FTIR) spectroscopy, energy dispersive X-ray spectroscopy (EDX), and X-ray diffraction (XRD) analysis showed the presence of biomolecules from the leaves extract, which was responsible for the productions of PO-AgNPs and the crystalline nature of the PO-AgNPs. Field emission scanning electron microscope (FESEM) images revealed the spherical structure of PO-AgNPs. Disc diffusion and time-kill assay results showed that PO-AgNPs exhibited inhibition against tested Methicillin-resistant *Staphylococcus aureus* (MRSA), *S. aureus*, and *S. epidermidis,* and *Pseudomonas aeruginosa*. Overall, these results further consolidate that PO-AgNPs possess good antibacterial properties. The inhibition mechanisms of PO-AgNPs against those pathogenic bacteria will be investigated in future works, particularly to explain how PO-AgNPs caused toxicity in bacteria.

INTRODUCTION

The emergence of green nanotechnology with promising biomedical applications has marked a new era in nanotechnology research, especially in manufacturing nanoparticles. Recent findings reported that green synthesized silver nanoparticles exhibit antibacterial activity against numerous microorganisms, including yeasts, bacteria, and fungi [1,2]. Likewise, numerous findings concluded that green synthesized silver nanoparticles exhibit a broad-spectrum antibacterial activity, suggesting an alternative agent for antibacterial resistance. To date, considerable research on the antibacterial effect of the green silver nanoparticles was carried out, yet there is still limited information on their inhibitory effects against skin-associated bacteria. Currently, reports on the inhibitory actions of silver nanoparticles against the bacteria tested were centered on the interaction of the nanoparticles and the bacterial membrane [1-4]. It was reported that the minute size of nanoparticles aids the attachment of the nanoparticles on the cell wall of the bacteria, hence facilitating the disruption of the membrane, which further leads to cell death.

Therefore, in this present study, the antibacterial effects of AgNPs prepared by using the leaves extract of *P. odorata* as the reducing agent were investigated. The formation of PO-AgNPs was first verified by characterization techniques to evaluate the physicochemical characteristics of the silver nanoparticles. The antibacterial activity of the green AgNPs against skin-associated bacteria was further evaluated by disc diffusion assay and time-kill curves.

International Conference on Life Sciences and Technology (ICoLiST 2020)
AIP Conf. Proc. 2353, 030022-1–030022-5; https://doi.org/10.1063/5.0052607
Published by AIP Publishing. 978-0-7354-4096-8/$30.00

EXPERIMENTAL DETAILS

Biosynthesis of PO-AgNPs

The leaves of *P. odorata* was cleaned with tap water twice to remove debris and organic contaminants, followed by deionized water and air-dried at room temperature for a week [5, 6]. The dried leaves were then grounded into fine powder form, then a concentration of 2% (w/v) of the extract was prepared [6]. The extract was left at room temperature to cool down and then filtered with Whatman filter paper no. 1. Synthesis of PO-AgNPs was carried out by adding 1 mL *P. odorata* leaves extract into 10 mL of 1 mM of $AgNO_3$. The reaction was allowed to stand for 24 hours in dark condition at room temperature to minimize the photo-activation of $AgNO_3$. Formation of PO-AgNPs was evidenced by the colour changes from yellowish to dark brown.

Physicochemical Properties of PO-AgNPs

The formation of PO-AgNPs was confirmed by UV-Visible spectrophotometer by measuring the spectrum in the range of 370 to 700 nm using a UV-Vis spectrophotometer (Jenway 7200). FTIR analysis was conducted by using FTIR Perkin-Elmer in the wavelength range of 4000 to 450 cm^{-1} to determine the present of pythochemical constituents in the leaf extract and its function in the reduction of PO-AgNPs. XRD analysis was conducted using a SmartLab X-ray diffractometer to evaluate the crystalline nature of the PO-AgNPs. The morphology and shape of the PO-AgNPs were assessed using FESEM (Hitachi SU8020).

Antibacterial Activity of PO-AgNPs

The antibacterial study was evaluated by the standard disc diffusion technique and time-kill assay. Briefly, sterile blank discs with a 6 mm diameter and 1 mm thick were impregnated with either 20 µL of 500 µg/mL PO-AgNPs or 30 µg/mL chloramphenicol (CHL), as a positive control. The discs were then placed on the Muller-Hinton agar plates, which were already swabbed with the bacteria and incubated for 24 hours at 37 °C. The antibacterial capacity of the PO-AgNPs was evaluated by measuring the inhibition zone around the discs as bacterial growth inhibition. This assay was conducted in triplicate. Time-kill assays were performed at MIC value for each bacterial strain to determine the rate at which a specific concentration of PO-AgNPs able to kill the bacterial isolate. Tubes containing MH broth (MHB), MHB with CHL, and MHB with PO-AgNPs were inoculated with the bacterial suspension at an initial density of 10^6 CFU/mL in a volume of 2 mL and incubated in a shaking incubator at 37 °C, 170 rpm. Aliquots of 100 µL were removed at specific times 0, 4, 6, 8, 10- and 24-hour post-inoculation. A 100 µL aliquot was diluted in a sterile 0.9 % sodium chloride solution, and an aliquot of 50 µL from the diluted sample were plated in triplicate on Muller-Hinton agar plates to determine the viable counts.

RESULTS AND DISCUSSION

Visible colour changes were observed from yellowish to brownish after two hours of adding the plant extract to the $AgNO_3$ solution, as shown in Figure 1(b). Over time, the colour intensity increased to dark brown, as shown in Figure 1(f). This observation is in accordance with other research findings that utilize plant extract as the reducing agent [7-10]. These observable changes signify the formation of AgNPs and can be visually observed through the naked eye due to the unique visible properties that AgNPs possess. AgNPs are known to emit colour ranging from reddish-brown to yellow [11].

FIGURE 1. The colour changes upon the addition of the plant extract to $AgNO_3$ at 0 (a), 2 (b), 4 (c), 6 (d), 8 (e), and 24 h (f).

From the UV-Vis spectra in Figure 2(a), it was known that the SPR for PO-AgNPs occurs at band 440 nm, aligned with other findings which suggested that AgNPs possess SPR band in the range of 430 – 450 nm. From the FTIR spectra in Figure 2(b), it can be observed that both *P. odorata* and PO-AgNPs have identical spectrum, with some marginal shifts in peaks and intensity suggesting that some residual moieties of the bioorganic compounds from *P. odorata* have formed complexes with the metal and stayed on the surface of the AgNPs. The FTIR spectra of *P. odorata* showed several absorbance bands at different locations, including 3432, 2924, 1632, 1446, and 1057 cm^{-1}, which proved the presence of organic acids phenols, and aliphatic amines in the *P. odorata* leaves extract, comparable to the FTIR spectra of PO-AgNPs at 3431, 2924, 1609, and 1056 cm^{-1}. These findings were also reported by others whose using leaves extract as the reducing agent [12-14]. From Figure 2(c), the XRD graph shows the presence of four peaks at 2θ values which corresponds to (1 1 1), (2 0 0), (2 2 0), (3 1 1), and (2 2 2) planes of silver respectively. From the diffractogram, the presence of several additional peaks that are unassigned can be observed, suggesting the presence of the crystallized bioorganic phase on the surface of the PO-AgNPs and further confirmed the UV-vis and FTIR analyses. This finding has also been observed in other studies [15, 16]. The surface morphology of the fabricated PO-AgNPs in Figure 2(d) indicates that the fabricated PO-AgNPs have a spherical shape. The EDX spectrum in Figure 2(e) shows an intense peak of elemental silver at 3 keV, and other peaks of C and O, which might be arisen due to the formation of the plant biomolecules onto the PO-AgNPs surfaces.

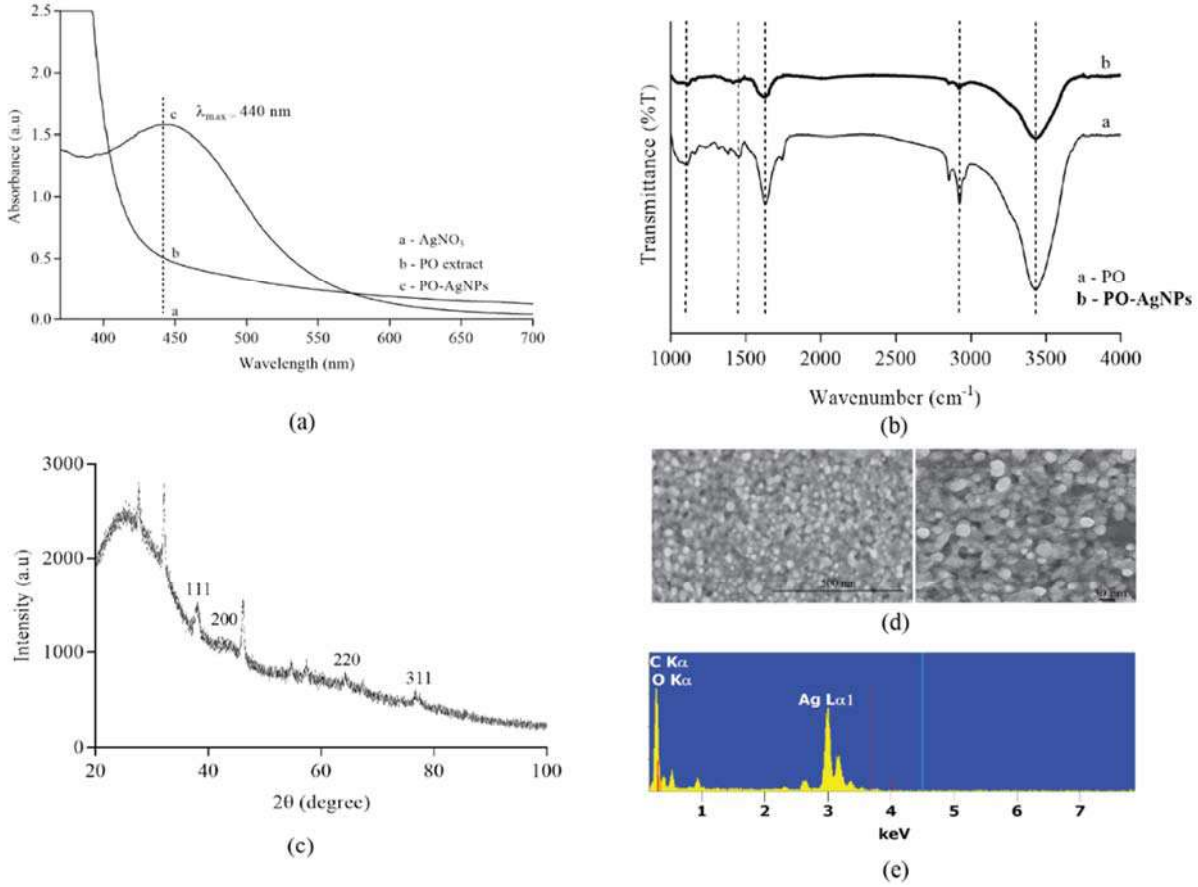

FIGURE 2. The synthesis of PO-AgNPs was confirmed using UV-vis spectrophotometer (a), FTIR spectrum (b), XRD analysis (c), FESEM images (d), and EDX analysis (e).

The antibacterial efficacy of PO-AgNPs against MRSA, *S. aureus, S. epidermidis,* and *P. aeruginosa* was first analyzed by the zone of inhibition, as shown in Table 1. This result demonstrated that PO-AgNPs possessed antibacterial activity against tested bacteria. From the result, it was observed that an increased amount of PO-AgNPs exhibited a greater inhibition zone.

TABLE 1. The inhibition zone of different bacteria treated with different amounts of PO-AgNPs. Data were presented as mean ± SD from three independent experiments (n = 3).

Tested material	Inhibition zone of tested bacteria (mm)			
	MRSA	***S. aureus***	***S. epidermidis***	***P. aeruginosa***
CHL	14 ± 0.17	18 ± 0.10	18 ± 0.29	9 ± 0.29
PO-AgNPs (10 μg)	7 ± 0.12	8 ± 0.06	10 ± 0.29	9 ± 0.06
PO-AgNPs (50 μg)	8 ± 0.61	9 ± 0.06	11 ± 0.58	10 ± 0.76
PO-AgNPs (200 μg)	11 ± 0.10	12 ± 0.58	13 ± 0.06	13 ± 0.06

To further evaluate the effect of PO-AgNPs against the growth of bacteria, killing experiments were conducted. From the time-kill curves in Figure 3, it can be concluded that the number of viable cells for each bacterium was reduced within 24 hours, indicating that PO-AgNPs was able to inhibit bacterial growth against all tested bacteria. From the curve, a potent inhibition was observed in *P. aeruginosa,* which might be due to the thin peptidoglycan layer, which further facilitates the interaction of PO-AgNPs against the bacteria.

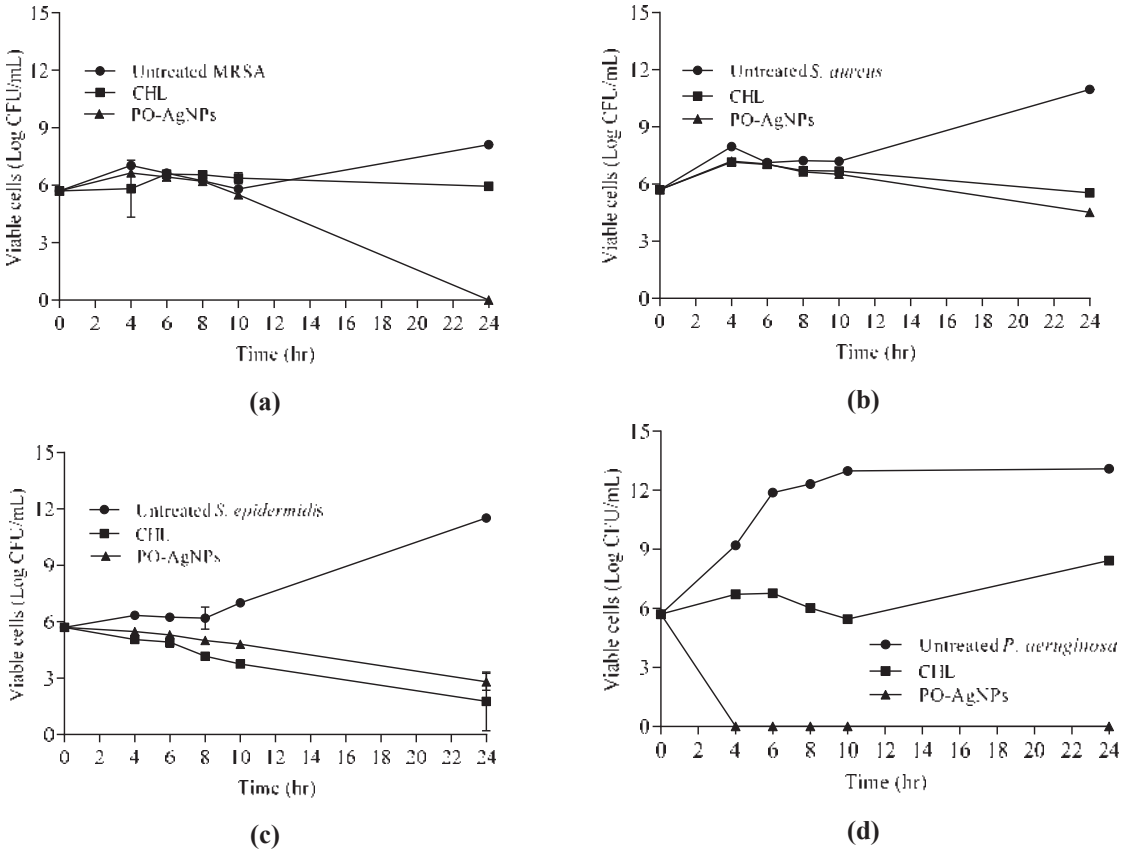

FIGURE 3. Time-kill curves for MRSA (a), *S. aureus* (b), *S. epidermidis (c),* and *P. aeruginosa* (d) against PO-AgNPs. Data were presented as mean ± SD from three independent experiments (n = 3).

SUMMARY

In conclusion, the findings of this study suggested that the green synthesis of AgNPs using leaves extract of *P. odorata* exhibited good antibacterial activities against MRSA, *S. aureus, S. epidermidis*, and *P. aeruginosa*. Considerable inhibitory effects were observed against MRSA, *S. aureus,* and *S. epidermidis*, whilst potent inhibitory activity was observed against *P. aeruginosa*. Although the present findings provide insight into the inhibition activities of PO-AgNPs against the tested bacteria, further studies are needed to understand the mechanistic of the PO-AgNPs as an antibacterial agent.

ACKNOWLEDGEMENTS

The authors would like to acknowledge Universiti Teknologi Malaysia (UTM) Transdisciplinary Research Grant (Grant No.: 06G86) for funding this research.

REFERENCES

1. K. Al-Dhafri and C. L. Ching, Biocatalysis and Agricultural Biotechnology **18**, 101075 (2019).
2. M. Maghimaa and S. A. Alharbi, Journal of Photochemistry and Photobiology B: Biology **204**, 111806 (2020).
3. B. Ajitha, Y. A. K. Reddy, H.-J. Jeon and C. W. Ahn, Advanced Powder Technology **29** (1), 86-93 (2018).
4. N. S. Alharbi, M. Govindarajan, S. Kadaikunnan, J. M. Khaled, T. N. Almanaa, S. A. Alyahya, M. N. Al-Anbr, K. Gopinath and A. Sudha, Journal of Trace Elements in Medicine and Biology **50**, 146-153 (2018).
5. S. Ahmed, M. Ahmad, B. L. Swami and S. Ikram, Journal of Radiation Research and Applied Sciences **9** (1), 1-7 (2016).
6. S. Borhamdin, M. Shamsuddin and A. Alizadeh, Journal of Experimental Nanoscience **11** (7), 518-530 (2016).
7. N. Ahmad, S. Sharma, M. K. Alam, V. Singh, S. Shamsi, B. Mehta and A. Fatma, Colloids and Surfaces B: Biointerfaces **81** (1), 81-86 (2010).
8. B. Ajitha, Y. A. K. Reddy and P. S. Reddy, Materials Science and Engineering: C **49**, 373-381 (2015).
9. S. A. AL-Thabaiti, Z. Khan and S. Hussain, Journal of Molecular Liquids **212**, 316-324 (2015).
10. A. Baghizadeh, S. Ranjbar, V. K. Gupta, M. Asif, S. Pourseyedi, M. J. Karimi and R. Mohammadinejad, Journal of molecular liquids **207**, 159-163 (2015).
11. V. Armendariz, M. Jose-Yacaman, A. Duarte Moller, J. Peralta-Videa, H. Troiani, I. Herrera and J. Gardea-Torresdey, Revista Mexicana de Fisica Supplement **50** (1), 7-11 (2004).
12. S. Hamedi, S. A. Shojaosadati and A. Mohammadi, Journal of Photochemistry and Photobiology B: Biology **167**, 36-44 (2017).
13. F. Mojab, M. Kamalinejad, N. Ghaderi and H. R. Vahidipour, Iranian Journal of Pharmaceutical Research (2), 77-82 (2010).
14. S. Oh, M. Jang, J. Kim, J. Lee, H. Zhou and J. Lee, Current Applied Physics **16** (7), 738-747 (2016).
15. M. R. Shaik, M. Khan, M. Kuniyil, A. Al-Warthan, H. Z. Alkhathlan, M. R. H. Siddiqui, J. P. Shaik, A. Ahamed, A. Mahmood and M. Khan, Sustainability **10** (4), 913 (2018).
16. A. Tripathy, A. M. Raichur, N. Chandrasekaran, T. Prathna and A. Mukherjee, Journal of Nanoparticle Research **12** (1), 237-246 (2010).